Nanoscale Res Lett (2009) 4:377–384
DOI 10.1007/s11671-009-9257-2

NANO EXPRESS

Effects of Growth Conditions on Structural Properties of ZnO Nanostructures on Sapphire Substrate by Metal–Organic Chemical Vapor Deposition

C. C. Wu · D. S. Wuu · P. R. Lin · T. N. Chen · R. H. Horng

Received: 4 December 2008 / Accepted: 8 January 2009 / Published online: 23 January 2009
© to the authors 2009

Abstract ZnO was grown on sapphire substrate by metal–organic chemical vapor deposition using the diethylzinc (DEZn) and oxygen (O_2) as source chemicals at 500 °C. Influences of the chamber pressure and O_2/DEZn ratio on the ZnO structural properties were discussed. It was found that the chamber pressure has significant effects on the morphology of ZnO and could result in various structures of ZnO including pyramid-like, worm-like, and columnar grain. When the chamber pressure was kept at 10 Torr, the lowest full width at half-maximum of ZnO (002) of 175 arc second can be obtained. On the other hand, by lowering the DEZn flow rate, the crystal quality of ZnO can be improved. Under high DEZn flow rate, the ZnO nanowall-network structures were found to grow vertically on the sapphire substrate without using any metal catalysts. It suggests that higher DEZn flow rate promotes three-dimensional growth mode resulting in increased surface roughness. Therefore, some tip on the ZnO surface could act as nucleation site. In this work, the growth process of our ZnO nanowall networks is said to follow the self-catalyzed growth mechanism under high-DEZn flow rate.

Keywords ZnO · Chamber pressure · O_2/DEZn ratio · Nanowall networks · Self-catalyzed

C. C. Wu · D. S. Wuu (✉) · P. R. Lin · T. N. Chen
Department of Materials Science and Engineering, National Chung Hsing University, Taichung 402, Taiwan, ROC
e-mail: dsw@dragon.nchu.edu.tw

R. H. Horng
Institute of Precision Engineering, National Chung Hsing University, Taichung 402, Taiwan, ROC

Introduction

ZnO is an attractive direct wide band gap (E_g ~3.36 eV at 300 K) semiconductor material for applications in the short wavelength light-emitting devices in the blue to ultraviolet (UV) region [1]. The interest in ZnO is fueled and fanned by its excellent properties such as good piezoelectric characteristics, chemical stability, and biocompatibility; and its potential applications in optoelectronics switches, near-UV lasers, and complex three-dimensional (3D) nanoscale systems [2, 3]. On the other hand, ZnO is also useful for many types of device such as surface acoustic wave devices, hydrogen-storage devices, transparent electrodes, transparent thin-film transistors, solar cells, and sensors [4–7]. Different methods have been used to synthesize various kinds of ZnO structures, for example, molecular beam epitaxy [8], metal–organic chemical vapor deposition (MOCVD) [9–11], thermal evaporation [12], and solution-phase process [13]. Among these techniques, MOCVD has been used for high quality epitaxial growth of various semiconductors and oxides, which is the ideal production technology for growth of epitaxial ZnO thin films. However, unlike the relatively mature MOCVD technique for III–V compound semiconductor growth, research into MOCVD growth of ZnO is still in its early stages. Since MOCVD is believed to be one of the complicated methods for the epitaxial growth of ZnO thin films, it will be necessary to investigate the effects of growth parameters, e.g., growth temperature, chamber pressure, and flow ratio of group VI source gas to group II source gas (VI/II). Effects of growth temperature have been discussed in our previous work [14]. This research is carried out to understand the structure and characteristics of ZnO grown on sapphire substrates under different chamber pressures and VI/II ratios. It was found that the ZnO

nanowall-network structures were found to grow vertically on the sapphire substrate without using any metal catalysts under high-DEZn flow rate. According to the energy spectrum analysis, the growth of ZnO nanowll networks is said to follow the self-catalyzed growth mechanism.

Experimental Details

The growth of ZnO was carried out by the MOCVD system reconstructed from the Emcore D-180 system. ZnO structure was deposited directly on the *c*-plane sapphire substrate. Diethylzinc (DEZn) and high-purity oxygen (O_2) gas were used as the zinc precursor and the oxidizer. DEZn vessel was immersed in the bubbler at 17 °C while the pressure of the DEZn source was kept at 350 Torr. The growth parameters include the chamber pressure and the ratio of oxygen and zinc. Ar gas was used as a carrier gas and the total gas flow including DEZn, O_2, and Ar in the chamber was fixed at 3000 sccm. The base parameters: growth temperature was 500 °C, oxygen flow rate was 600 sccm, Ar gas flow rate through the DEZn vessel was 20 sccm, rotation of disk was 1000 rpm, and growth time was 60 min. First of all, we changed the chamber pressure from 10 to 60 Torr. Then, the ratio of oxygen and zinc was adjusted from 200 to 500. At last, the flow of Ar gas through the DEZn vessel was changed from 10 to 40 sccm with the oxygen gas fixed at 600 sccm. The thickness of ZnO structure was measured using a Tencor-KLA (P-10) profilometer. X-ray diffraction (XRD; X'Pert Pro MRD) in the θ–2θ and rocking curve mode was carried out to identify the crystal quality and orientation of ZnO structure. The Cu Kα line ($\lambda = 1.541874$ Å) was used as the source and Ge (220) was used as the monochromator. The cross-sectional morphologies of ZnO structure were observed by scanning electron microscopy (SEM; Hitachi S-300H). The energy spectra were observed by field emission scanning electron microscopy/energy-dispersive X-ray spectroscopy (FE-SEM/EDS; JEOL JSM-6700F/ OXFORD INCA ENERGY 400). The surface roughness of ZnO was analyzed using atomic force microscopy (AFM; Agilent 5400 AFM/SPM) and the measurements were accomplished with a Si cantilever for contact AFM, and the scan speed and scan area were 0.5 µm/s and 5×5 µm^2, respectively. The photoluminescence (PL) was measured at room temperature by 325 nm line of a He–Cd laser (8 mW) as the excitation source.

Results and Discussion

The growth rate of ZnO on sapphire substrate using DEZn and O_2 sources under different chamber pressures is shown in Fig. 1. The growth rate decreased with increasing chamber pressure because the thickness of the boundary layer increased with increasing chamber pressure. The thicker the boundary layer, the harder the atoms diffuse onto the growing surface. By reducing the chamber pressure, the gas flows on the sample surface became more stable. The diffusivities of these gases increased with decreasing chamber pressure and therefore the growth rate increased. Figure 2a–f shows the SEM images of ZnO grown at different chamber pressures from 10 to 60 Torr. In Fig. 2a and b, the morphologies of ZnO are columnar grain and worm-like structure. With increasing chamber pressure, the ZnO structures become pyramid-like grain and the grain size decreases as shown in Fig. 2c–e. As shown in Fig. 2f, ZnO do not uniformly grow on the sapphire substrate because the gas molecules may pre-react in the air before absorbing onto the substrate. The gas phase reaction causes the generation of particles and results in a high surface roughness of the sample. The gas flow should be kept in the laminar flow regime to achieve stable flow in the chamber. For this reason, the chamber pressure used in this work was reduced in order to achieve stable flow and reduce the pre-reaction.

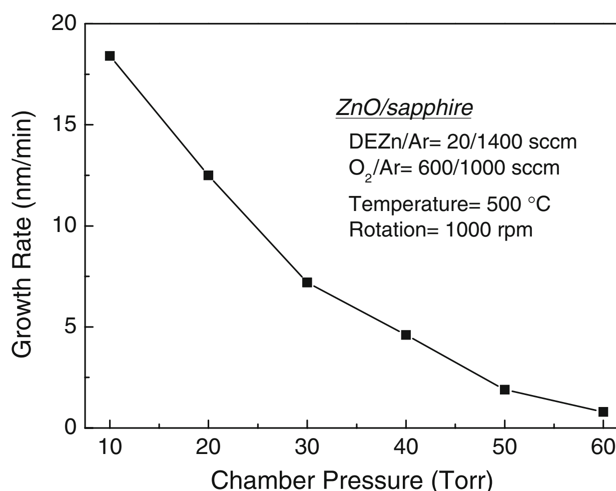

Fig. 1 Growth rate of ZnO as a function of chamber pressure

Double crystal XRD analysis was used for further investigation. As shown in Fig. 3, the XRD of ZnO grown at various chamber pressures ranging from 10 to 60 Torr is studied. At 60 Torr, the peak of XRD intensity is not found. At 50 Torr, the intensity of (002) and (101) diffraction peaks appear. At 40 Torr, the ZnO peak intensity of (002) and (101) were nearly the same. With decreasing chamber pressure from 40 to 10 Torr, the (101) peak of ZnO intensity feebly emerged while the (002) diffraction peak of ZnO intensity increased gradually. Inset Fig. 3 shows the rocking curve profile at the (002) spectrum of ZnO grown at various chamber pressures. At 10 Torr, the

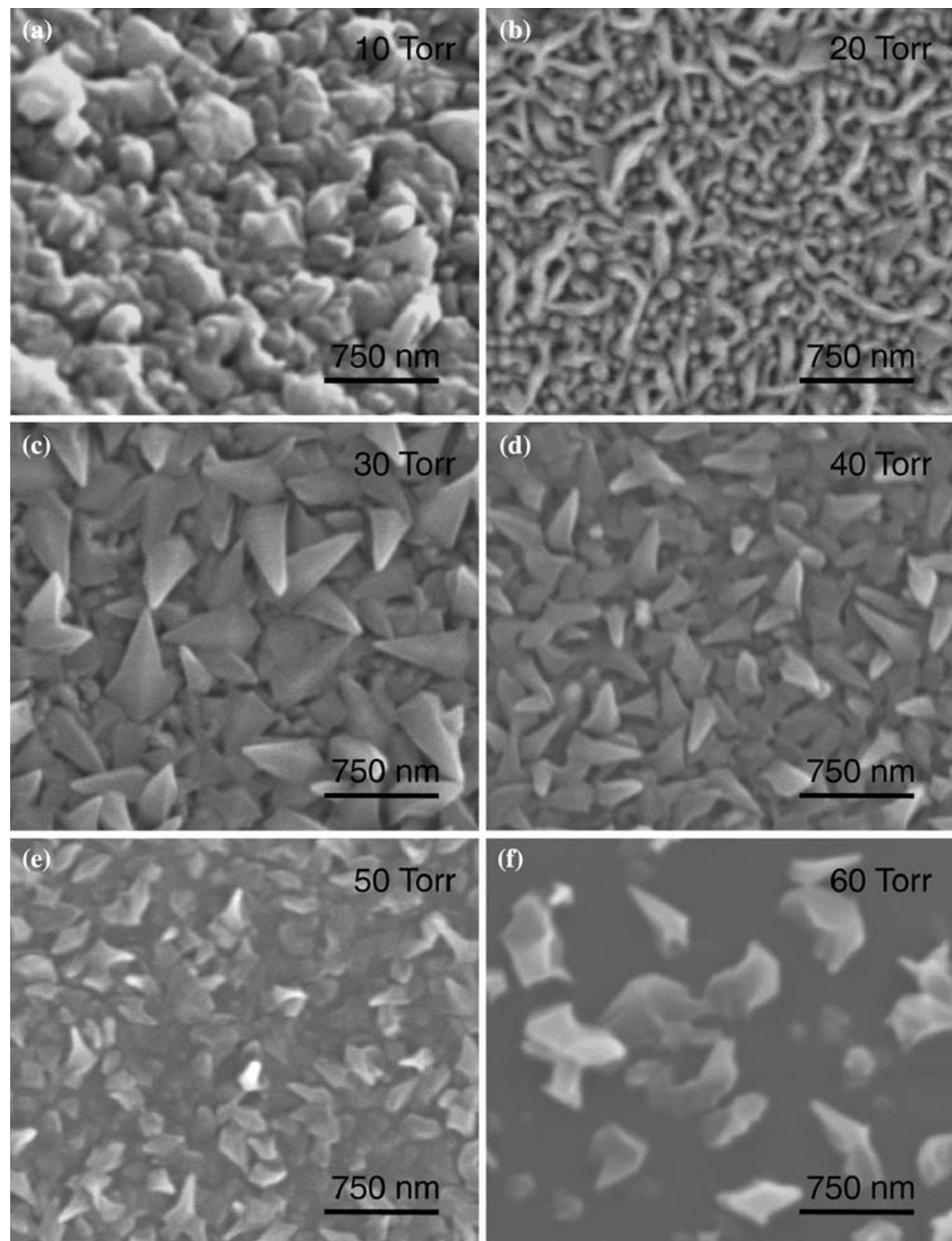

Fig. 2 SEM images of ZnO grown on sapphire substrate at different chamber pressures: **a** 10, **b** 20, **c** 30, **d** 40, **e** 50, and **f** 60 Torr

intensity of ZnO (002) diffraction was strong with the full width at half-maximum (FWHM) value of 175 arc second. The small FWHM can be obtained with the ZnO grown at lower chamber pressure. The reduced crystal quality at the chamber pressure above 10 Torr suggests that the boundary layer starts to become thick, leading to less adsorption of reactants onto the surface, thus reducing the growth rate and crystal quality. As shown in Fig. 2f, higher pressures may lead to turbulent flow on the surface and therefore induces a non-uniform growth.

As shown in Fig. 4, PL measurements were performed at room temperature in order to investigate the optical properties of ZnO. All of the ZnO samples exhibited UV emissions while a peak energy position of near 3.2 eV was dominantly observed. The FWHM values of the UV peak varied from 151 to 123 meV with decreasing chamber pressure from 60 to 10 Torr. In addition, a very strong blue peak can be observed in the spectrum of ZnO grown at higher chamber pressure. The UV peak is said to result from the near band emission (NBE) while the blue peak results from the deep-level emission (DLE). The formation of DLE is ascribed to native defects such as zinc interstitial, oxygen vacancy, and zinc vacancy [15–17]. This suggests that, with increasing pressure, the concentration of zinc interstitials increases because the higher reactor pressure suppresses desorption of Zn from the surface, leading to Zn-rich conditions on the surface [18]. Therefore, this indicates that better optical properties can be

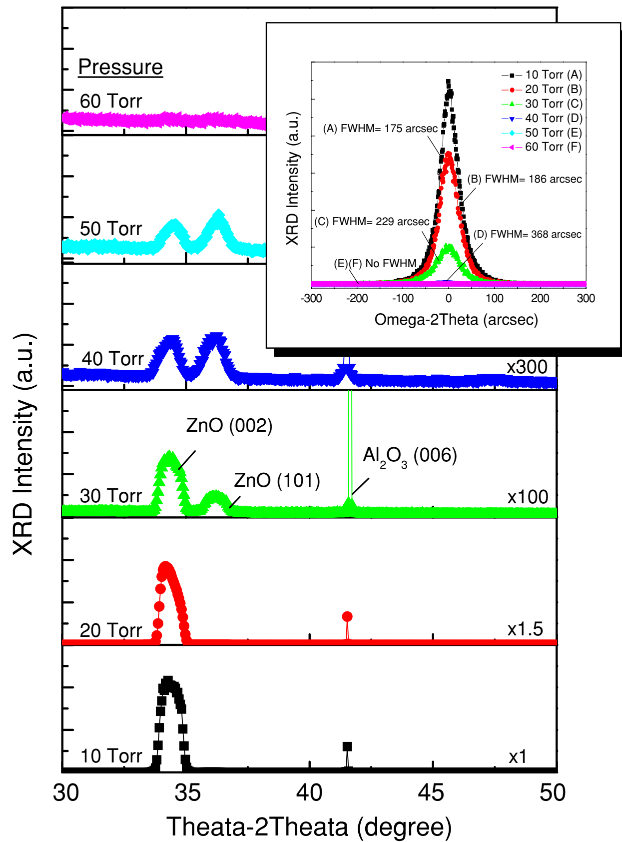

Fig. 3 Double crystal XRD θ–2θ pattern of ZnO grown at the pressure ranging from 10 to 60 Torr. Inset figure shows the XRD rocking curve profile at the (002) reflection of ZnO as a function of chamber pressure

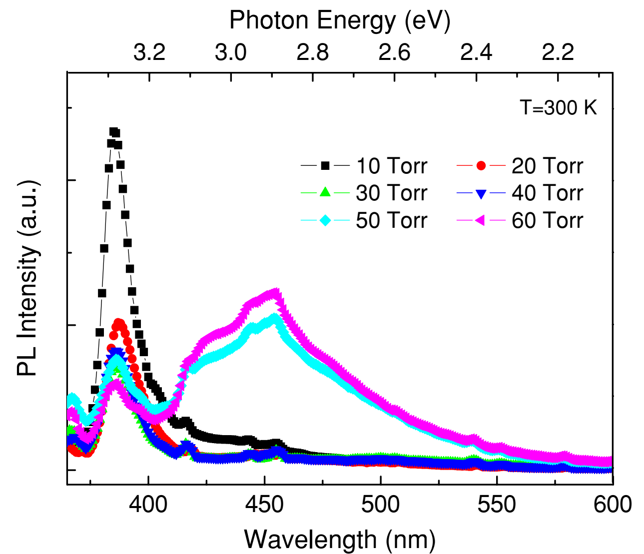

Fig. 4 Room temperature PL spectra of ZnO grown at the pressure range of 10–60 Torr

obtained by lowering the chamber pressure. According to the SEM, XRD, and PL results, we chose to grow ZnO at a relatively low chamber pressure of 10 Torr.

Effects of VI/II (O_2/DEZn) ratio on the surface morphology and crystal quality of ZnO on the sapphire substrates have been investigated. The VI/II ratio was varied by changing the DEZn flow rates from 10 to 40 sccm, while the O_2 flow rate was fixed at 600 sccm. The SEM images of ZnO grown at different DEZn flow rates

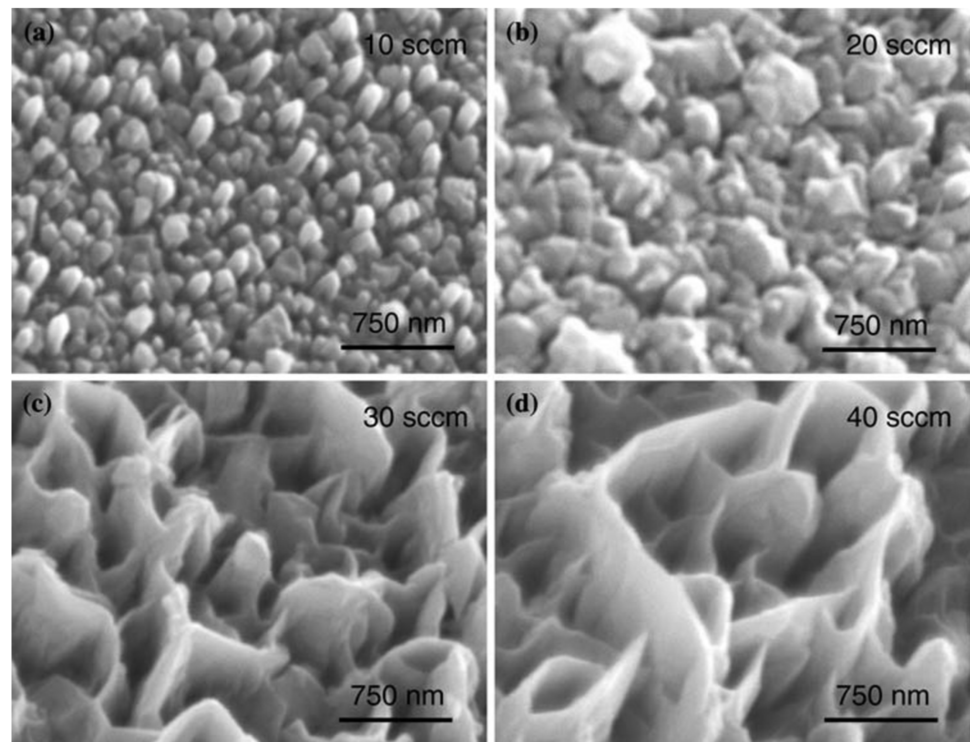

Fig. 5 SEM images of ZnO grown on sapphire substrate at different DEZn flow rates: **a** 10, **b** 20, **c** 30, and **d** 40 sccm

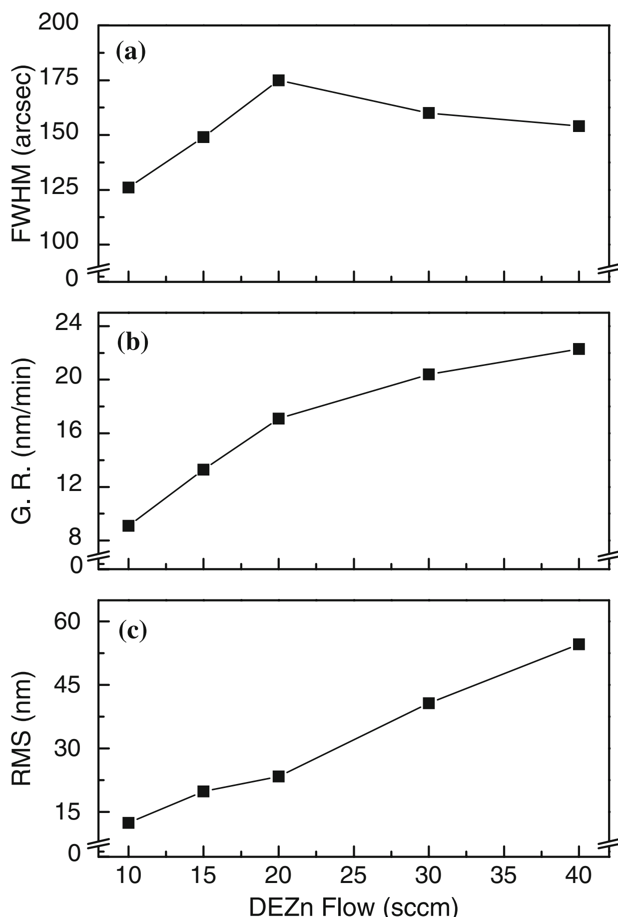

Fig. 6 **a** FWHM of XRD rocking curve profile at the (002) spectrum, **b** growth rate, and **c** surface roughness of ZnO grown at different DEZn flow rates in the range from 10 to 40 sccm

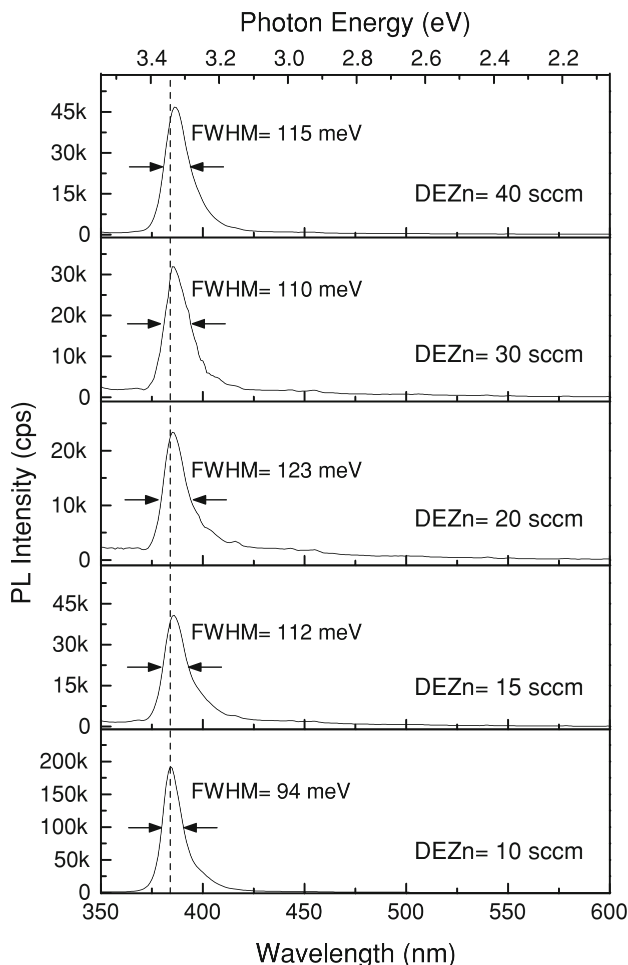

Fig. 7 Room temperature PL spectra of ZnO grown at different DEZn flow rates from 10 to 40 sccm

are shown in Fig. 5a–d. In Fig. 5a and b, the morphologies of ZnO are columnar grain while the average grain size increases with increasing DEZn flow rate. In Fig. 5c and d, ZnO structures become nanowall-network structures with increasing DEZn flow rate above 30 sccm. The same tendency was found in the size of nanowall-network structures. The size of the nanowall-network structures increases with increasing DEZn flow rates from 30 to 40 sccm. The influences of DEZn flow rate on the crystal quality, growth rate, and surface roughness of ZnO were investigated and shown in Fig. 6. In Fig. 6a, the FWHM of (002) ZnO rocking curves are 126, 149, and 175 arc second while the DEZn flow rates are 10, 15 and 20 sccm, respectively. However, FWHM values became small when the DEZn flow rate increased from 20 to 40 sccm due to the transformation of ZnO structure from columnar grain-like structure to nanowall networks with increasing DEZn flow rate. The improved crystal quality is caused by the better *c*-axis-oriented growth of nanowall-network structure. It was found that the DEZn/O_2 ratio could have a significant effect on the morphology and structure of ZnO while it only had small effect on the crystal quality of ZnO. In Fig. 6b and c, with increasing DEZn flow rate from 10 to 40 sccm, the growth rate increases from 9.1 to 22.3 nm/min while the surface smoothness deteriorates from 12.4 to 54.6 nm. This indicates that ZnO tends to grow in a 3D mode under high-DEZn flow rate resulting in increase surface roughness and the formation of the nanowall-network structures [19]. According to these results, 1D growth and columnar structures form under higher VI/II ratio while 3D growth becomes dominant factor under lower VI/II ratio.

Room temperature PL spectra of ZnO structures were measured in order to compare the optical properties of ZnO grown at different DEZn flow rates. As shown in Fig. 7, the PL intensity of NBE increased remarkably with decreasing DEZn flow rate. Meanwhile, the FWHM values are 94, 112, 123, 110, and 115 meV while the DEZn flow rates are 10, 15, 20, 30 and 40 sccm, respectively. This result corresponds to the XRD phenomena as show in Fig. 6a and it suggests that the better optical quality can be obtained on

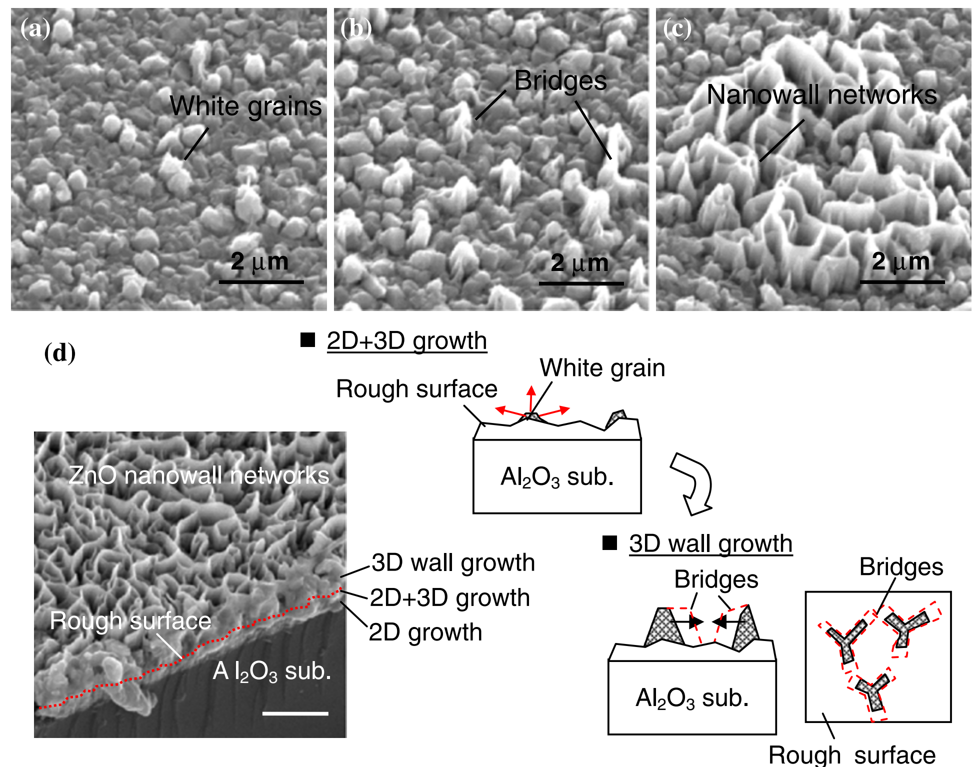

Fig. 8 SEM images of ZnO nanowall networks grown at different growth times of **a** 25, **b** 30, and **c** 35 min. **d** Schematic illustration of the growth mechanism of ZnO nanowall networks grown on sapphire substrate without using any metal catalysts. Inset image shows the SEM result of nanowall networks grown at 60 min with the scale bar of 2.5 μm

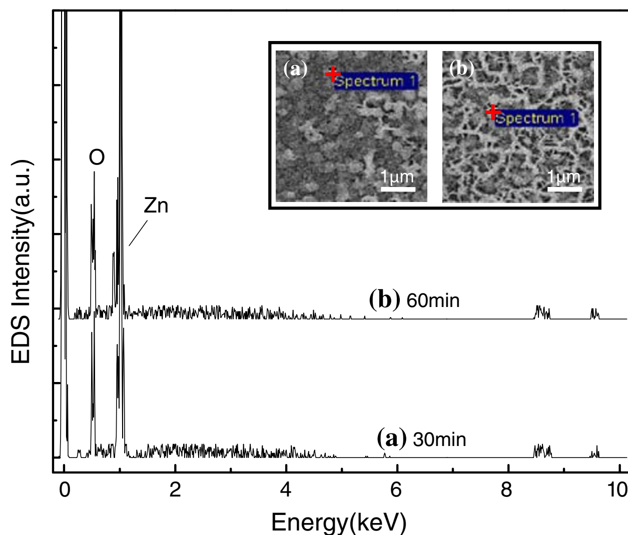

Fig. 9 EDS results of ZnO nanowall-network structure grown at (a) 30 and (b) 60 min. The inset figures show the FE-SEM images of ZnO nanowall-network structure grown at **a** 30 and **b** 60 min

the present condition by reducing the DEZn flow rate to 10 sccm. In addition, the peak position shifts to short wavelength (high energy) with decreasing DEZn flow rate. It was reported that the shift of band gap energy relates to the change of strain [20, 21]. The band gap energy decreased from 3.23 to 3.20 eV with increasing DEZn flow rate from 10 to 20 sccm, indicating the relaxation of strain. It may play a key role in the formation of ZnO nanowall networks because this relaxation process can give rise to lateral growth of (100) and (101) orientation resulting in the formation of wall structure.

In the past years, vapor–liquid–solid (VLS) has been used to explain the growth mechanisms of ZnO nanostructures [22–27]. In 2003, Ng et al. have demonstrated that the formation of nanowall networks was based on a VLS growth mode by using Au as catalyst and the growth temperature was very high (~925 °C) [22]. Moreover, related research of ZnO nanowall networks via metal catalysts have been reported by many other research groups since then [23, 24]. The VLS growth mechanism has been widely used to explain the formation of ZnO nanowall-network structure. Au, Cu, Ni, and Sn were used as the typical metal catalysts in these researches. However, in this work, the ZnO nanowall networks can be obtained at a relatively low temperature around 500 °C without using any metal catalysts. It is expected to increase the versatility and power of these building blocks for nanoscale photonic and electronic device applications. To better understand the growth mechanism, ZnO nanowall networks on the sapphire substrate were prepared at different time intervals of 25, 30, and 35 min for further investigation. Figure 8 shows a series of SEM images for clarifying the growth mechanism of ZnO nanowall network. As shown in Fig. 8a, continuous grains are observed at the initial stage. With increasing growth time, the surface starts to become

rough and the rough grains (white grain) start to connect with each other by bridges (Fig. 8b). Finally, vertical ZnO nanowall networks are formed directly on sapphire substrate (Fig. 8c). Figure 8d shows the schematic illustration of the ZnO nanowall networks growth mechanism. Owing to the lattice mismatch between ZnO and sapphire substrate, ZnO do not obey a two-dimensional layer-by-layer growth mode. Under high-DEZn flow rate, the 3D growth mode causes increasing surface roughness. The tip on the ZnO surface could work as an activation site for the formation of the ZnO nanowall networks because of the different surface energy. The ZnO structure tends to form at the tips of the ZnO surface to reduce the local surface energy [28, 29]. To investigate the growth behavior of the ZnO nanowall networks, energy spectrum analyses were conducted. Figure 9 shows the composition of ZnO nanowall networks grown at different growth times of 30 and 60 min measured by the EDS equipped on the FE-SEM. Inset figure show the ZnO structure grown at 30 and 60 min with the FE-SEM measured regions marking by the "red cross". It is clear that, at the growth time of 30 or 60 min, the nanowall networks is composed of Zn and O. The EDS analysis did not reveal any metal catalysts or any other type of additives on ZnO nanowall-network structure. It suggested that the growth of ZnO nanowall networks follows the self-catalyzed growth mechanism which is different from the common VLS mechanism.

Conclusion

The structure and morphology of ZnO was found to vary with the chamber pressure and the ratio of zinc and oxygen. By lowering the chamber pressure to 10 Torr and the DEZn flow rate to 10 sccm, the crystal and optical properties of ZnO can be improved. Under high-DEZn flow rate, the ZnO nanowall-network structures were found to grow vertically on the sapphire substrates without using any metal catalysts. This indicates that the ZnO grows in a 3D growth mode under higher DEZn flow rate. The 3D growth mode causes increasing surface roughness and thus forming the vertical ZnO nanowall networks. The tip on the ZnO surface may act as "nucleation site" to form nanowall-network structures following the self-catalyzed growth mechanism. The formation mechanism of the ZnO nanowall networks is different from the previous reports which use metal as catalysts.

Acknowledgments This work was supported by the National Science Council and Ministry of Economic Affairs, Taiwan, Republic of China, with Grant Nos. NSC95-2221-E-005-131-MY3 and 97-EC-17-A-07-S1-097, respectively.

References

1. B.Y. Man, C. Yang, H.Z. Zhuang, M. Liu, X.Q. Wei, H.C. Zhu et al., J. Appl. Phys. **101**, 093519 (2007). doi:10.1063/1.2730573
2. Z.W. Pan, Z.R. Dai, Z.L. Wang, Science **291**, 1947 (2001). doi:10.1126/science.1058120
3. H.L. Zhou, S.J. Chua, H. Pan, J.Y. Lin, Y.P. Feng, L.S. Wang et al., Electrochem. Solid-State Lett. **10**, H98 (2007). doi:10.1149/1.2428413
4. N. Ohashi, K. Kataoka, T. Ohgaki, T. Miyagi, H. Haneda, K. Morinaga, Appl. Phys. Lett. **83**, 4857 (2003). doi:10.1063/1.1632030
5. Q. Wan, C.L. Lin, X.B. Yu, T.H. Wang, Appl. Phys. Lett. **84**, 124 (2004). doi:10.1063/1.1637939
6. S.J. Young, L.W. Ji, S.J. Chang, Y.K. Su, J. Cryst. Growth **293**, 43 (2006). doi:10.1016/j.jcrysgro.2006.03.059
7. H.Y. Tsai, J. Mater. Process. Technol. **192–193**, 55 (2007). doi:10.1016/j.jmatprotec.2007.04.029
8. B.P. Zhang, N.T. Binh, Y. Segawa, K. Wakatsuki, N. Usami, Appl. Phys. Lett. **83**, 1635 (2003). doi:10.1063/1.1605803
9. G. Du, Y. Ma, Y. Zhang, T. Yang, Appl. Phys. Lett. **87**, 213103 (2005). doi:10.1063/1.2132528
10. D.C. Kim, B.H. Kong, H.K. Cho, J. Mater. Sci: Mater. Electron. **19**, 760 (2008). doi:10.1007/s10854-007-9404-4
11. K. Black, A.C. Jones, P.R. Chalker, J.M. Gaskell, R.T. Murray, T.B. Joyce et al., J. Cryst. Growth **310**, 1010 (2008). doi:10.1016/j.jcrysgro.2007.11.131
12. H. Wang, Z.P. Zhang, X.N. Wang, Q. Mo, Y. Wang, J.H. Zhu et al., Nanoscale Res. Lett. **3**, 309 (2008). doi:10.1007/s11671-008-9156-y
13. J. Grabowska, A. Meaney, K.K. Nanda, J.P. Mosenier, M.O. Henry, J.R. Duclere et al., Phys. Rev. B **71**, 115439 (2005). doi:10.1103/PhysRevB.71.115439
14. C.C. Wu, D.S. Wuu, T.N. Chen, T.E. Yu, P.R. Lin, R.H. Horng et al., J. Nanosci. Nanotechnol. **8**, 3851 (2008). doi:10.1166/jnn.2008.181
15. Y. Chen, Y. Pu, L. Wang, C. Mo, W. Fang, B. Xiong et al., Mater. Sci. Semicond. Process. **8**, 491 (2005). doi:10.1016/j.mssp.2004.07.006
16. B. Cao, W. Cai, H. Zeng, Appl. Phys. Lett. **88**, 161101 (2006). doi:10.1063/1.2195694
17. D. Yu, L. Hu, J. Li, H. Hu, H. Zhang, Z. Zhao et al., Mater. Lett. **62**, 4063 (2008). doi:10.1016/j.matlet.2008.04.079
18. M. Pan, W.E. Fenwick, M. Strassburg, N. Li, H. Kang, M.H. Kane et al., J. Cryst. Growth **287**, 688 (2006). doi:10.1016/j.jcrysgro.2005.10.093
19. S.W. Kim, S. Fujita, M.S. Yi, D.H. Yoon, Appl. Phys. Lett. **88**, 253114 (2006). doi:10.1063/1.2216107
20. Y. Ma, G.T. Du, T.P. Yang, D.L. Qiu, X. Zhang, H.J. Yang et al., J. Cryst. Growth **255**, 303 (2003). doi:10.1016/S0022-0248(03)01244-2
21. H.S. Kang, J.S. Kang, J.W. Kim, S.Y. Lee, J. Appl. Phys. **95**, 1246 (2004). doi:10.1063/1.1633343
22. H.T. Ng, J. Li, M.K. Smith, P. Nguyen, A. Cassell, J. Han et al., Science **300**, 1249 (2003). doi:10.1126/science.1082542
23. J.S. Jeong, J.Y. Lee, J.H. Cho, C.J. Lee, S.J. An, G.C. Yi et al., Nanotechnology **16**, 2455 (2005). doi:10.1088/0957-4484/16/10/078
24. S.W. Kim, H.K. Park, M.S. Yi, N.M. Park, J.H. Park, S.H. Kim et al., Appl. Phys. Lett. **90**, 033107 (2007). doi:10.1063/1.2430918
25. A. Reiser, A. Ladenburger, G.M. Prinz, M. Schirra, M. Feneberg, A. Langlois et al., J. Appl. Phys. **101**, 054319 (2007). doi:10.1063/1.2710295

26. L.L. Yang, J.H. Yang, D.D. Wang, Y.J. Zhang, Y.X. Wang, H.L. Liu et al., Phys. E **40**, 920 (2008). doi:10.1016/j.physe.2007.11.025
27. S.R. Hejazi, H.R. Madaah Hosseini, M. Sasani Ghamsari, J. Alloy Comp. **455**, 353 (2008). doi:10.1016/j.jallcom.2007.01.100
28. P.X. Gao, C.S. Lao, Y. Ding, Z.L. Wang, Adv. Funct. Mater. **16**, 53 (2006). doi:10.1002/adfm.200500301
29. Z. Yin, N. Chen, R. Dai, L. Liu, X. Zhang, X. Wang et al., J. Cryst. Growth **305**, 296 (2007). doi:10.1016/j.jcrysgro.2007.04.043